Biomedicine & Pharmacotherapy 202 (2026) 119736

Contents lists available at ScienceDirect

Biomedicine & Pharmacotherapy

journal homepage: www.elsevier.com/locate/biopha

Development and characterization of [^{47}Sc]Sc-NOTA-trastuzumab for targeted radiotherapy in primary and metastatic HER2 + breast cancer

Patrick N. Song [a,b,1], Shelbie J. Cingoranelli [a,c,1], Sharmila Sridhar [a], Hailey A. Houson [a,c], Carlos A. Gallegos [a,d], Lily B. Watts [a], Jennifer L. Bartels [c], Christopher D. Willey [e,f], Suzanne E. Lapi [a,c,f,1,*], Anna G. Sorace [a,d,f,1,**]

[a] Department of Radiology, The University of Alabama at Birmingham, Birmingham, USA
[b] Graduate Biomedical Sciences, The University of Alabama at Birmingham, Birmingham, USA
[c] Department of Chemistry, The University of Alabama at Birmingham, Birmingham, USA
[d] Department of Biomedical Engineering, The University of Alabama at Birmingham, Birmingham, USA
[e] Department of Radiation Oncology, The University of Alabama at Birmingham, Birmingham, USA
[f] O'Neal Comprehensive Cancer Center, The University of Alabama at Birmingham, Birmingham, USA

ARTICLE INFO

Keywords:
Theranostic
SPECT
CT
Metastasis
Immune modulation

ABSTRACT

Purpose: This study investigates the potential of [^{47}Sc]Sc-NOTA-trastuzumab as a novel targeted radionuclide agent in HER2 + breast cancer. Targeted radionuclide therapy offers a promising approach for enhanced delivery and internalization of radiation, minimizing off-target effects and treating advanced metastatic HER2 + breast cancers. By examining the synergistic relationship between [^{47}Sc]Sc with trastuzumab, assessing [^{47}Sc]Sc-NOTA-trastuzumab's impact on immune function, and monitoring its passage of a compromised blood-brain barrier for targeting HER2 + breast-to-brain metastases, this study provides a path towards synergistic and precision radiotherapy in breast cancer metastasis.

Experimental Design: The stability, specificity and reactivity of [^{47}Sc]Sc-NOTA-trastuzumab was characterized with high performance liquid chromatography, Lindmo, and cell binding assays. *In vivo* localization and therapeutic efficacy were assessed with SPECT imaging, biodistribution, and tumor monitoring in models of HER2 + breast cancer. Immunostaining against M1 macrophages was assessed to determine mechanisms of enhanced anti-tumoral immune activity.

Results: [^{47}Sc]Sc-NOTA-trastuzumab demonstrates high specificity and serum stability in HER2 + cells. SPECT shows [^{47}Sc]Sc-NOTA-trastuzumab has high specificity for HER2 + breast cancer cells *in vivo* in both the primary and metastatic setting. Longitudinally, tumors treated with [^{47}Sc]Sc-NOTA-trastuzumab show therapeutic benefit and are comparable to those treated with 16x dose of trastuzumab alone, with no significant toxicity. Exploratory results show radiopharmaceutical uptake in a model of HER2 + brain metastasis. Increased M1-like macrophages were seen in HER2 + tumors relative to HER2- tumors following treatment with [^{47}Sc]Sc-NOTA-trastuzumab.

Conclusion: [^{47}Sc]Sc-NOTA-trastuzumab is serum stable and highly specific to HER2 + breast cancer. Developing and characterizing novel targeted radionuclide therapeutics has the potential to significantly improve radionuclide delivery in HER2 + metastatic disease.

1. Introduction

Identifying novel approaches to target molecular biomarkers on tumor surfaces and enabling immune cells to recognize and attack tumors is a critical area of focus in nuclear medicine [1]. Trastuzumab (Herceptin) is a humanized IgG mAb that binds the human epidermal

* Correspondence to: Department of Radiology and Chemistry, The University of Alabama at Birmingham, 1824 6th Ave S, Birmingham, Alabama 35233, USA.
** Correspondence to: Department of Radiology and Biomedical Engineering, The University of Alabama at Birmingham, 1670 University Blvd, Birmingham, Alabama 35233, USA.
E-mail addresses: lapi@uab.edu (S.E. Lapi), asorace@uabmc.edu (A.G. Sorace).
[1] Denotes equal contribution.

https://doi.org/10.1016/j.biopha.2026.119736
Received 2 April 2026; Received in revised form 8 June 2026; Accepted 2 July 2026
Available online 21 July 2026
0753-3322/© 2026 The Authors. Published by Elsevier Masson SAS. This is an open access article under the CC BY-NC license (http://creativecommons.org/licenses/by-nc/4.0/).

growth factor receptor 2 (HER−2)/neu [2] and has been previously conjugated to radionuclides to allow for PET or SPECT imaging [3–5]. HER2-targeted PET imaging, especially with radiotracers like [^{89}Zr]Zr-DFO-trastuzumab, has enabled characterization of HER2 + metastases across multiple lesions [6–8]. Clinical trials using [^{89}Zr]Zr-DFO-trastuzumab show the agent localizes within HER2 + brain metastases, underscoring its utility in identifying primary and metastatic sites that are surgically difficult to resect [5]. These findings highlight the potential of HER2 PET imaging as a powerful diagnostic tool and as a means of guiding individualized therapeutic interventions and in HER2 + lesions.

Standard-of-care treatment for HER2 + breast cancer is stage dependent, but includes surgery, anti-HER2 trastuzumab, radiation therapy, and chemotherapy. In the metastatic setting, antibody-drug-conjugates have emerged as a promising therapeutic strategy that combines the selectivity of monoclonal antibodies with the cytotoxic potency of chemotherapy [9]. Additional combination therapies have been explored and it has also been shown that trastuzumab synergizes with radiation in both preclinical and clinical studies [10–12]. Ahmed *et al.* observed that combination trastuzumab, pertuzumab and radiation therapy increases overall survival in patients with HER2 + leptomeningeal disease [13]. These studies were conducted using external beam irradiation to induce this synergistic effect in solid tumors and significantly reduced tumor viability. However, due to the limitations of external beam therapy, radiation cannot be delivered to each individual metastatic site. Targeted radiotherapy is a promising approach used clinically for neuroendocrine and prostate cancer [14–18] and is in numerous ongoing preclinical and clinical trials across other cancer types [19–21] to delivery targeted radiation therapy to metastatic lesions systemically.

Theranostic strategies in oncology leverage diagnostic imaging to identify patients likely to benefit from radionuclide therapy and to monitor response [22]. Targeted radionuclide therapy delivers ionizing radiation to cancer cells via directly radiolabeled monoclonal antibodies (mAbs) [23], enabling precise targeting of metastatic lesions. Several therapeutic radionuclides have been conjugated with trastuzumab, including ^{111}In, ^{131}I, ^{212}Pb and ^{177}Lu [24–26]. Among these, only ^{177}Lu and ^{212}Pb have reached clinical trials [24,27]. Combining mAbs, which exhibit high specificity to antigens overexpressed on the tumor cell with radionuclides for therapies, creates a dual theranostic approach to treat cancer [28,29]. While the concept of incorporating therapeutic radionuclides with trastuzumab is not new, no such compound has yet received FDA approval, highlighting a need for further exploration into dosing strategies, isotope selection, localization of therapeutic mAb-radionuclides to metastatic sites, and understanding the synergistic effects of radionuclide-emitted radiation [23].

Incorporating elementally matched radionuclides for both the diagnostic and therapeutic radiopharmaceutical would yield compounds with identical pharmacokinetics, pushing this approach towards a more personalized medicine as the chemically identical diagnostic compound could be used to predict the intratumoral uptake and distribution of the therapeutic compounds, especially in models where small radiochemical changes alter biodistribution [30,31]. The advantage of [^{47}Sc]Sc comparable to many current β-emitting radioisotope (e.g. [^{177}Lu]Lu) is its triad of medically relevant scandium nuclides suitable for imaging, [^{43}Sc]Sc, [^{44}Sc]Sc, with potential for elementally matched pairs [32–34]. This study is the first investigation into the therapeutic potential of [^{47}Sc]Sc in breast cancer, thereby evaluating the potential of [^{47}Sc]Sc-NOTA-trastuzumab as a potential radioimmunotherapy agent in HER2 positive breast cancer. Further, this work explores the *in vitro* and *in vivo* synergic potential between [^{47}Sc]Sc ionizing radiation with trastuzumab, evaluates alterations in innate immune response, and explores the potential of targeting HER2 + brain metastases.

2. Materials and methods

All chemicals were trace metal grade or analytical. Water was obtained from an 18.2 MΩ-cm water purification system (Milli-Q System, Millipore, Billerica, MA) and interacted with Chelex resin (Bio-Rad, Hercules, CA) for 24 h prior to filtration. Trastuzumab (Herceptin™) was purchased from Genentech (South San Francisco, CA). Human and mouse serum was sourced from EMD Millipore Corporation (Temecula, CA). *P*-SCN-Bn-NOTA was purchased from Macrocyclics (Plano, TX). Zeba™ Spin Desalting Columns, 40 K MWCO, 0.5 mL were purchased from ThermoFisher Scientific. HEPES, carbonate and ammonium acetate were purchased from Sigma Aldrich.

2.1. Cell culture and tumor models

Human HER2 + cell lines, BT474 and SKBR3, and human HER2- cell lines, MDA MB 231 and MDA MB 468, were acquired from ATCC. The BT474 cell line was maintained in Improved Modified Eagle's Media (IMEM) supplemented with 10% Fetal Bovine Serum (FBS) and 0.5% Insulin. The SKBR3, MDA MB 231 and MDA MB 468 cell lines were maintained in Dulbecco's Modified Eagle's Media (DMEM) supplemented with 10% FBS, 1% Sodium Pyruvate and 1% L-Glutamine. Cell lines tested negative for pathogens through Charles River Research Animal Diagnostic Services. Cells were used within 10 passages from the stock vial to maintain biological validity.

All animal procedures were performed in accordance with The University of Alabama at Birmingham's Institutional Animal Care and Use Committee (APN 21611). Five- to six-week-old female athymic nude mice were obtained from Charles River Laboratories (Catalog number: 490). To establish subcutaneous models, 1×10^7 BT474 cells or 2×10^6 MDA MB 231 cells were engrafted with 30% Matrigel and 70% serum free media. To establish intracranial models, 5×10^5 BT474 cells were intracranially engrafted at the right hemisphere of the brain. To establish intracardiac models, 5×10^5 BT474 were intracardiacally engrafted into the right ventricle of athymic nude mice.

2.2. Synthesis and radiochemistry of [^{47}Sc]Sc-NOTA-trastuzumab

Preparation of NOTA-trastuzumab was conducted similar to previous literature [35,36]. *P*-SCN-Bn-NOTA was conjugated with buffer-exchanged anti-human HER2 antibody trastuzumab in a 10:1 molar ratio in 0.1 M carbonate buffer pH 9, for 2 h at 37 °C. The reaction was purified using Zeba Spin columns (150 kD) to yield NOTA-trastuzumab in 1 M HEPES pH7. After conjugation and purification, final NOTA-trastuzumab stocks were quantified using a BCA assay. The assumed molecular weight for NOTA-trastuzumab was 146, 897.2 g/mol [36]. Scandium−47 was obtained from the University of Alabama at Birmingham Cyclotron facility, produced via the vanadium production route previously described [32,37,38]. The ^{47}Sc was evaporated to dryness before being brought up in 0.25 M ammonium acetate pH 5.5 (25 μL). 100–175 μg NOTA-trastuzumab was added and the reaction was incubated at 37 °C for 30 min. The final activity of the labeled complex was 1.5 – 2.5 mCi (55.5 – 92.5 MBq). Complexation was determined using instant thin-layer chromatography (iTLC-SG) developed in 50 mM EDTA pH 5.5 and analyzed using Eckert & Ziegler AR−2000 radio-TLC scanner and WinScan software (Hopkinton, MA). Here, [^{47}Sc]Sc-NOTA-Trastuzumab remained at the baseline, RF = 0, while [^{47}Sc]$ScCl_3$ moved with the solvent front, RF = 1 [32,33]. For stability assays, [^{47}Sc]Sc-NOTA-trastuzumab was incubated in 1 mL of either human serum, mouse serum or PBS, at 37 °C, 800 RPM, and % complexation was analyzed using iTLC throughout 14 d.

2.3. Assessing [^{47}Sc]Sc-NOTA-trastuzumab's immunoreactivity in vitro

The immunoreactivity of [^{47}Sc]Sc-NOTA-trastuzumab was assessed using Lindmo et al. assay in HER2 + BT474 cells as described in Omweri

et al. [4,39]. Cellular uptake assays and internalizations were performed in HER2 + BT474 and HER2- MDA-MB−468. 2.5 × 10^5 cells in 1 mL of media were incubated in 12 well plates, 24 h prior to study. After incubation, media was removed, and cells were incubated with 145 ng of [^{47}Sc]Sc-NOTA-trastuzumab in 1 mL of media for both cellular uptake or internalization. Cell binding assay involved BT474 or MDA MB 231 cells that were incubated with [^{47}Sc]Sc-NOTA-trastuzumab for 2 h at 37 °C. After incubation, the media was removed, cells were washed with PBS and lysed with 0.2 M NaOH. Blocking studies used 100 μg in 1 mL of unlabeled NOTA-trastuzumab, incubated 10 min prior. The lysate was measured on a HIDEX gamma counter. After counting, a BCA assay was performed for total protein concentration. The internalization study used only BT474 cells. After the addition of [^{47}Sc]Sc-NOTA--trastuzumab, cells were incubated at 0.25, 0.5, 0.75, 1, 2, 4, 6 and 24 h. After incubation, cells were washed with PBS, washed with cold 0.1 M citric acid and then lysed with 0.2 M NaOH. Both the citric acid fraction and NaOH fraction were measured on a gamma counter. Results were calculated by the percentage of activity in each fraction compared to the sum of citric and lysate fractions. Immunoreactive fraction was calculated through linear extrapolation of total/bound activity versus inverse normalized cell concentration, where the reciprocal of the y-intercept corresponds to the immunoreactive fraction [39].

2.4. Assessing the retention of [^{47}Sc]Sc-NOTA-trastuzumab in HER2 + breast cancer cells in vitro

To assess retention of [^{47}Sc]Sc-NOTA-trastuzumab, a Western blot and autoradiography assay was performed. BT474, SKBR3 and MDA MB 231 cells were treated with saline control, trastuzumab (0.2 μg/mL), [^{47}Sc]$ScCl_3$ (4 μCi/mL), or [^{47}Sc]Sc-NOTA-trastuzumab (4 μCi/mL or 0.148 MBq/mL) for 24 h, prior to being lysed for Western blot. Cell lysate was run for western blot, incubated with primary and secondary antibody and developed against autoradiography film for 2 h using the Typhoon Biomolecular Imager. Following autoradiography, the membrane was developed with Pierce ECL Western Blot Substrate (Fisher Scientific Catalog #: 32209) and visualized with CL-XPosure Film (Fisher Scientific Catalog #: 34089).

2.5. Assessing in vitro cytotoxicity and retention of [^{47}Sc]Sc-NOTA-trastuzumab through colony forming assay

To assess changes in clonogenic survival of HER2 + cells during treatment to [^{47}Sc]Sc-NOTA-Trastuzumab, a clonogenic assay was performed. BT474 cells were treated with control, trastuzumab (1 μg/mL), [^{47}Sc]$ScCl_3$ (250 μCi or 9.25 MBq), or [^{47}Sc]Sc-NOTA-trastuzumab (250 μCi) for 1 h. Following treatment, cells were trypsinized and seeded on a 6-well plate at a ratio of 10,000 cells/well. Cells were allowed to grow undisturbed in a humidified incubator (37 C and 5% CO_2) for 14 d. After 14 d, cells were fixed with 10% formalin for 30 min and stained with crystal violet for 60 min. Following staining, cells were visualized with the EVOS M7000. Colonies, of at least 20 cells, were quantified through Matlab code (R2024b, Mathworks, Natick, MA) [40].

2.6. [^{47}Sc]Sc-NOTA-trastuzumab SPECT Imaging

Mice were engrafted with either HER2 + BT474 tumors or HER2- MDA MB 231 tumors and enrolled into imaging studies. At the time of imaging, BT474 tumors were 212.4 ± 50.5 mm^3 and MDA MB 231 tumors were 139.2 ± 33.1 mm^3. Mice were injected intravenously with 150 μCi or 5.55 MBq of [^{47}Sc]Sc-NOTA-Trastuzumab and imaged 6 h, and at 1-, 3-, 5-, and 7-d post radiotracer injection with a preclinical Single Photon Emission Computed Tomography (SPECT)/CT (U-SPECT^6-μCT-OI, MiLabs, Heidelberglaan, Netherlands). Mice were imaged for 1 h with SPECT followed by a CT for anatomical reference. On day 7, mice were euthanized post imaging for biological validation through biodistribution and immunohistochemistry. For biodistribution, immediately after imaging, tumors and select organs were collected, weighed and analyzed in a gamma counter to measure radioactivity. For this experiment, N = 5 BT474 tumors, N = 3 BT474 tumors were co-injected with blocking agent, N = 3 MDA MB 231 tumors and N = 3 MDA MB 231 tumors were co-injected with blocking agent into the [^{47}Sc]Sc-NOTA-Trastuzumab imaging experiment. SUV analysis was conducted through VivoQuant (Invicro, Boston, MA) and tumor volume corrections were applied. Regions of interest were manually drawn on CT and overlaid onto SPECT imaging. SUV was determined through the following formula:

$$SUV = \frac{radioactive\ concentration}{injected\ activty/body\ weight}$$

To assess the biodistribution of [^{47}Sc]Sc-NOTA-trastuzumab in metastatic models, mice were engrafted with HER2 + brain metastases through intracranial or intracardiac injection. For intracranial models of brain metastasis, BT474-Luc (Cellomics Technologies. Catalog Number: SC−1227) positive cells were implanted intracranially on the right hemisphere of a 5–6 week old female athymic nude mouse (N = 3) and enrolled into experiment ~8 weeks post injection. Tumor growth was monitored through bioluminescence imaging (BLI) with IVIS Lumina III (Perkin Elmer, Waltham, MA). Mice with an average BLI of at least 1 × 10^9 were enrolled into imaging experiments (Supplemental Fig. 3). Monitoring of tumor growth was measured through BLI and MRI on a biweekly basis. Co-localization of MRI and SPECT imaging was performed using VivoQuant's (Invicro, Boston, MA) Brain Atlas and semi-automated rigid registration workflows. Briefly, SUV_{peak} analysis was quantified as the 9 intersecting voxels with the highest average SUV within the ROI as previously described [41,42].

2.7. Assessing therapeutic response to [^{47}Sc]Sc-NOTA-trastuzumab in vivo

To assess the therapeutic potential of [^{47}Sc]Sc-NOTA-trastuzumab, HER2 + BT474 tumor bearing mice were treated with [^{47}Sc]Sc-NOTA-trastuzumab and monitored for long term changes in tumor viability. Mice were engrafted with 1 × 10^7 BT474 cells with 30% serum free matrigel and enrolled into the experiment when tumors grew to 150–200 mm^3. Mice were injected with either saline control, [^{47}Sc]Sc-NOTA-trastuzumab, or trastuzumab (one cohort of matched targeted radiotherapy dose (0.6 mg/kg), one cohort of clinically relevant therapeutic dose (10 mg/kg)). Mice were injected with 250 μCi or 9.25 MBq of [^{47}Sc]Sc-NOTA-trastuzumab on day 0 and day 30 via intravenous injection. Tumors were measured thrice weekly to assess for longitudinal changes in tumor viability until day 90.

2.8. Immunostaining of macrophage markers and verification of HER2 staining

Following SPECT imaging, tumors were excised for biological validation and stained against HER2, CD86 and trastuzumab. Briefly, tumors were fixed, sectioned and stained for HER2 (Cell Signaling Technologies, Catalog #: 2242), CD86 (Thermofisher, Catalog #: MA5–44065), and trastuzumab (Biotechne, Catalog #: MAB95471–100). Following staining, sections were digitized with an EVOS M7000 and quantified as percent positive stain through custom MATLAB code [43–46]. HER2 expression was quantified via QuPath image analysis software. A Gaussian filter was applied to smooth the image and reduce noise before cell detection. Nuclei were identified using the Hematoxylin stain and identified as regions with an optical density (OD) greater than 0.1. Size thresholds ensured that the nuclear area was between 25 and 400 μm to exclude debris or any major artifacts. After nuclei were identified, cytoplasm area was simulated by expanding the nuclear boundary by 2 μm in every direction, defining cell boundaries. DAB stain was used to quantify HER2 expression within individual cells. Initial thresholding established any cell region

containing a mean DAB OD greater than 0.195 as positive. Positive cells were filtered further using DAB maximum OD, or the maximum OD within any individual pixel. All cells with a DAB maximum OD greater than 0.75 within the cell boundary were classified as cells with positive HER2 expression.

2.9. Statistical analysis

Experimental conditions were summarized by average of replicates and error is represented by standard error of mean (SEM). Significance between experimental conditions was assessed using a Wilcoxon-rank-sum test. All data and figures were analyzed and generated using GraphPad Prism 7 (La Jolla, CA, USA).

3. Results

3.1. [^{47}Sc]Sc-NOTA-Trastuzumab maintains high specificity and reactivity in HER2 + breast cancer

The [^{47}Sc]Sc-NOTA-trastuzumab had a molar activity of 15 ± 1.3 μCi/μg (or 80.7 MBq/nmol). Following radiolabeling, the purity of [^{47}Sc]Sc-NOTA-trastuzumab exceeded 99% via instant thin-layer chromatography (iTLC) (Fig. 1A). Stability studies demonstrated that [^{47}Sc]Sc-NOTA-trastuzumab remained > 99% intact in PBS, human serum,

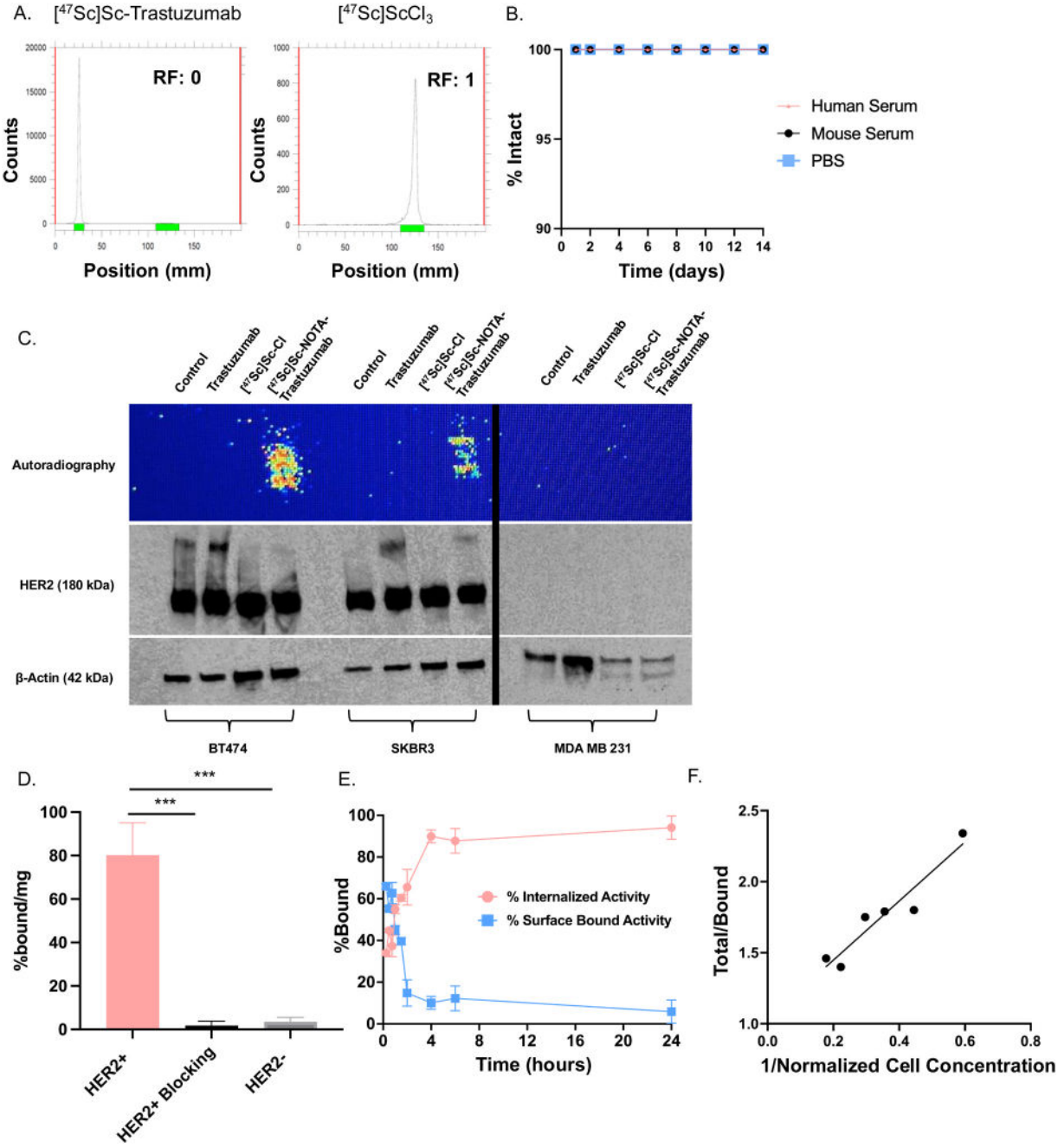

Fig. 1. [^{47}Sc]Sc-NOTA-trastuzumab exhibits high stability, specificity and immunoreactivity to HER2. iTLC analysis reveals approximately 100% labeling of trastuzumab when labeled at a ratio of 15 μCi/μg (A). HPLC analysis revealed 99 + % stability of [^{47}Sc]Sc-NOTA-trastuzumab in saline, human serum and mouse serum over the course of 14 days (B). Western blotting and autoradiography of [^{47}Sc]Sc-NOTA-trastuzumab reveals retention of [^{47}Sc] radioactivity was only observed in cells treated with [^{47}Sc]Sc-NOTA-trastuzumab (C). [^{47}Sc]Sc-NOTA-trastuzumab was observed to be highly specific and internalize in HER2 + cell lines (D, E). When normalized to cell concentration, an immunoreactivity assay identified 97% immunoreactivity of [^{47}Sc]Sc-NOTA-trastuzumab (F).

and mouse serum over a 14-d period (Fig. 1B). Western blot and autoradiography analysis qualitatively demonstrated retention of radioactivity in HER2-positive cells treated with [^{47}Sc]Sc-NOTA-trastuzumab, supporting HER2-associated retention of the radiotracer (Fig. 1C, Supplementary Fig. 1). A cell binding assay and internalization analysis were performed to determine the specificity and binding efficacy of [^{47}Sc]Sc-NOTA-trastuzumab in HER2-positive (with and without a blocking agent) and HER2-negative cell lines. Binding efficacy was determined to be 80.2 ± 14.8% in HER2-positive cells, which significantly decreased to 1.7 ± 1.9% upon treatment with 1.45 μg of cold trastuzumab ($p < 0.01$). Conversely, binding efficacy in HER2-negative cells was markedly reduced with a binding of 3.5 ± 2.0% ($p < 0.01$) (Fig. 1D). Internalization studies over 24 h demonstrated that [^{47}Sc]Sc-NOTA-trastuzumab internalized rather than remaining surface-bound, indicating rapid internalization in HER2-positive BT474 cells (Fig. 1E). Finally, a Lindmo assay revealed that [^{47}Sc]Sc-NOTA-trastuzumab retained 97% immunoreactivity (IRF = 0.969, $R^2 = 0.905$) when assessed against HER2 + breast cancer cells (Fig. 1 F).

3.2. [^{47}Sc]Sc-NOTA-Trastuzumab significantly decreases clonogenic survival in HER2 + breast cancer

To examine the survival of HER2 + breast cancer cells following targeted [^{47}Sc]Sc-NOTA-trastuzumab therapy, *in vitro* clonogenic survival was examined following 1 h of exposure to [^{47}Sc]Sc-NOTA-trastuzumab therapy. HER2 + breast cancer cell line (BT474) was treated with [^{47}Sc]$ScCl_3$, trastuzumab or [^{47}Sc]Sc-NOTA-trastuzumab therapy for 1 h prior to being plated for clonogenic survival (Fig. 2 A). Following 14 days, clonogenic survival of [^{47}Sc]Sc-NOTA-trastuzumab treated cells was determined to be significantly reduced, compared to [^{47}Sc]$ScCl_3$ alone or trastuzumab alone ($p < 0.01$) (Fig. 2B). With downstream changes in survival, coupled with high radiochemical purity, stability, specificity, and reactivity, [^{47}Sc]Sc-NOTA-trastuzumab was determined to be an effective treatment, outperforming either independent therapy, for HER2 + breast cancer cells *in vitro* and was determined to be suitable for *in vivo* assessment.

3.3. [^{47}Sc]Sc-NOTA-Trastuzumab exhibits high in vivo specificity with high clearance of normal organs

To investigate the *in vivo* therapeutic potential of [^{47}Sc]Sc-NOTA-trastuzumab, *in vivo* localization was assessed in HER2 + BT474 tumor-bearing mice. Significant uptake of [^{47}Sc]Sc-NOTA-trastuzumab was observed in HER2 + BT474 tumors (SUV_{mean}=9.1), while pre-treatment with 100 μg of cold trastuzumab markedly reduced tumor uptake in blocking groups (SUV_{mean} =1.2) ($p < 0.01$) (Fig. 3A). In contrast, HER2-MDA-MB−231 tumors, both untreated (SUV_{mean} =0.70) and blocked (SUV_{mean} =0.67), demonstrated minimal accumulation of [^{47}Sc]-NOTA-trastuzumab on day 7 ($p = 0.97$). In HER2 + tumors, the SUV_{mean} in the tumors and tumor-to-heart SUV ratio stabilized by day 3 and remained consistent through day 7 (Figs. 3B, 3C). Immunohistochemical analysis of excised tumors confirmed elevated HER2 expression in BT474 tumors relative to MDA-MB−231 tumors, consistent with imaging results (Figs. 3D, 3E). Immunohistochemical analysis was validated with western blot against human breast cancer cell lines (Supplemental Figure 4) and against published literature [43]. Analysis of muscle and heart SUV revealed low uptake of [^{47}Sc]Sc-NOTA-trastuzumab in muscle throughout the 7-day period, while heart uptake peaked within 24 h post-injection before clearing by day 7 ($p < 0.01$) (Supplemental Fig. 2). Biodistribution studies in normal organs indicated elevated uptake in the spleen and liver. Administration of cold trastuzumab significantly reduced tumor uptake of [^{47}Sc]Sc-NOTA-trastuzumab compared to unblocked tumors ($p < 0.0001$) (Fig. 4A) with no toxicity observed longitudinally, as indicated by an absence of weight loss across all groups (Fig. 4B).

3.4. [^{47}Sc]Sc-NOTA-Trastuzumab exhibits high in vivo therapeutic efficacy

To evaluate the therapeutic potential of [^{47}Sc]Sc-NOTA-trastuzumab, a separate cohort of BT474 tumor-bearing mice was administered two doses of [^{47}Sc]Sc-NOTA-trastuzumab (250 μCi or 9.25 MBq) on day 0 and day 30 and monitored over 60 day (Fig. 5A). Mice demonstrated no signs of toxicity during [^{47}Sc]Sc-NOTA-trastuzumab targeted radiotherapy as there was no significant change in weight. Because the therapeutic response of [^{47}Sc]Sc-NOTA-trastuzumab was equivalent to cold trastuzumab at a dose 16.6 times higher, we investigated the biological mechanisms underlying the antitumor activity of [^{47}Sc]-NOTA-trastuzumab. Immunohistochemical staining for CD86, and trastuzumab revealed increased anti-tumoral inflammation in HER2 + tumors treated with [^{47}Sc]Sc-NOTA-trastuzumab compared to HER2- tumors treated with [^{47}Sc]Sc-NOTA-trastuzumab (Fig. 5B). Control HER2 + BT474 tumors had 46.1 ± 9.6% trastuzumab binding, while control HER2- MDA MB 231 tumors had 6.1 ± 3.9% trastuzumab binding ($p < 0.01$). Control HER2 + BT474 tumors had 37.0 ± 16.5% CD86 expression, while control HER2- MDA MB 231 tumors had 7.4 ± 4.1% CD86 expression ($p < 0.01$).

3.5. Preliminary assessment of [^{47}Sc]Sc-NOTA-Trastuzumab delivery to HER2 + brain lesions

Having established the specificity and stability of [^{47}Sc]Sc-NOTA-trastuzumab *in vitro* and *in vivo*, we proceeded to evaluate its effectiveness in HER2 + metastatic breast-to-brain lesions. In the intracranial model, T_2-weighted MRI was conducted prior to the injection of [^{47}Sc]Sc-NOTA-trastuzumab. Since HER2 + breast-to-brain metastases are

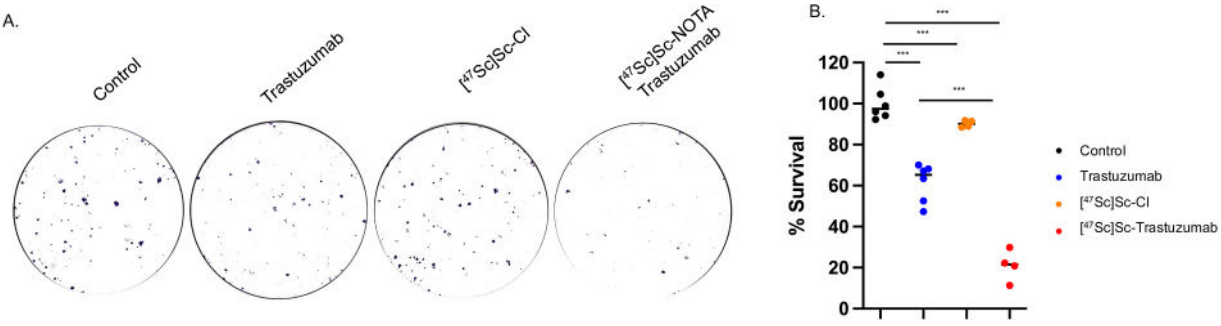

Fig. 2. [^{47}Sc]Sc-NOTA-trastuzumab significantly decreases clonogenic survival of HER2 + breast cancer *in vitro*. BT474 (HER2 +) cells were treated with [^{47}Sc]$ScCl_3$, trastuzumab or [^{47}Sc]Sc-NOTA-trastuzumab and survival was assessed with colony forming assay (A). Longitudinal survival suggests [^{47}Sc]Sc-NOTA-trastuzumab significantly decreases survival of HER2 + breast cancer cells relative to control and single agent treatment groups, outperforming either independent therapy, for HER2 + breast cancer cells *in vitro* (B).

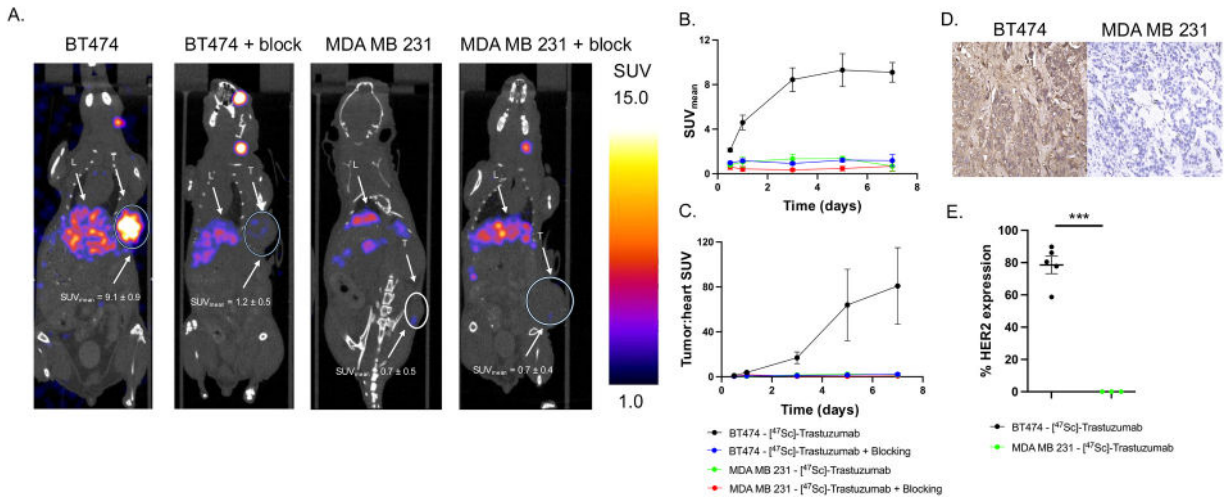

Fig. 3. SPECT imaging of [^{47}Sc]Sc-NOTA-trastuzumab reveals uptake is retained and stable *in vivo*. BT474 (HER2 +) or MDA MB 231 (HER2-) tumor bearing mice were engrafted and imaged with static single photon emission computed tomography (SPECT) imaging on day 7 (A). Quantitative analysis of [^{47}Sc]Sc-NOTA-trastuzumab retention reveals that [^{47}Sc]Sc-NOTA-trastuzumab uptake stabilizes in HER2 + tumor bearing mice beginning on d 3 (B). In HER2 + tumor bearing mice, [^{47}Sc]Sc-NOTA-trastuzumab tumor:heart ratio increases over the course of 7 days, suggesting clearance of [^{47}Sc]Sc-NOTA-trastuzumab in the heart while retention in the tumor remains consistent (C). Biological immunohistochemical validation against HER2 (D) reveals significant increased expression of HER2 in BT474 tumors relative to MDA MB 231 tumors (E). "T" denotes tumor and "L" denotes liver.

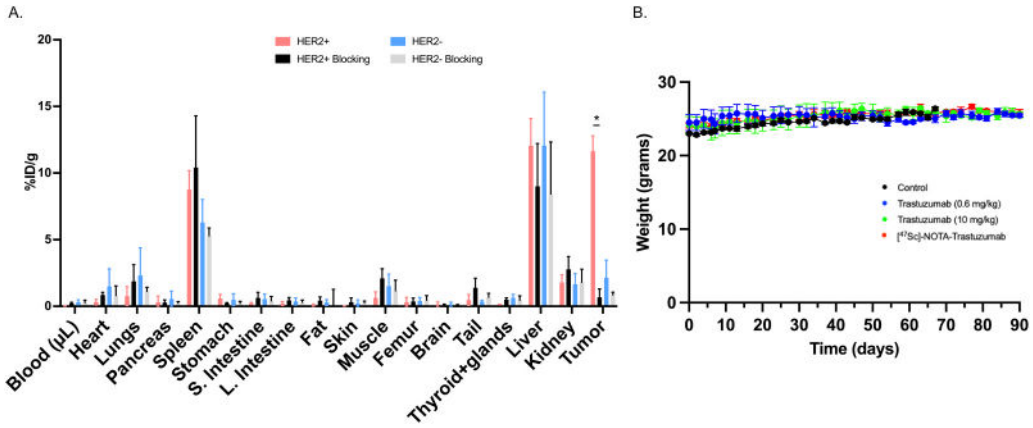

Fig. 4. Biodistribution of [47Sc]Sc-NOTA-trastuzumab shows tumor-specific uptake with minimal off-target retention and no evidence of systemic toxicity. Biodistribution analysis of select organs reveals the spleen and liver observe the highest uptake of [^{47}Sc]Sc-NOTA-trastuzumab in the body however no changes in uptake are observed among tumor groups. Biodistribution data does show significant increased [^{47}Sc]Sc-NOTA-trastuzumab retention in BT474 tumors relative to BT474 + block tumors (A). No significant changes in mouse weight was observed over the course of 60 days, suggesting [^{47}Sc]Sc-NOTA-trastuzumab is well tolerated (B).

common, we aimed to quantify therapeutic strategies targeting metastatic lesions. Notably, HER2 + intracranial models exhibited clear uptake of [^{47}Sc]Sc-NOTA-trastuzumab, co-registering with regions of HER2 + brain metastases (Figs. 6A, 6B). Analysis of [^{47}Sc]Sc-NOTA-trastuzumab SUV_{peak} in the brain revealed increased uptake of [^{47}Sc]Sc-NOTA-trastuzumab in HER2 + intracranial tumor bearing mice, relative to non-intracranial tumor bearing mice ($p = 0.03$) (Fig. 6B). Similarly, intracardiac HER2 + breast-to-brain lesions were engrafted and assessed for accumulation of [^{47}Sc]Sc-NOTA-trastuzumab through SPECT imaging and biodistribution (Fig. 6C). HER2 + intracardiac models exhibited a trending significant increase of [^{47}Sc]Sc-NOTA-trastuzumab in HER2 + intracardiac brain lesions compared to non-intracardiac tumor bearing mice ($p = 0.12$) (Fig. 6D). Similarly, biodistribution analysis reveals increased uptake of [^{47}Sc]Sc-NOTA-trastuzumab in intracardiac injected mice at organs such as the lung and spine, areas consistent with metastatic breast disease (Figs. 6E, 6F).

4. Discussion

This study is the first of its kind to explore the development and therapeutic potential of [^{47}Sc]Sc-NOTA-trastuzumab in breast cancer, including imaging of the delivery of the radiotargeted therapy to both primary and models of brain metastasis with SPECT. We demonstrate that [47Sc]Sc-NOTA-trastuzumab induces significant tumor growth inhibition with enhanced cytotoxic efficacy compared to trastuzumab alone, exhibits enhanced therapeutic effects relative to either radionuclide or antibody monotherapy and achieves comparable therapeutic efficacy to a 16-fold higher dose of trastuzumab while promoting a pro-inflammatory tumor microenvironment characterized by increased M1-like macrophage infiltration. In late stage HER2 + breast cancer, brain metastases can occur in up to 50% of patients [47], with only 20% of patients surviving one year following diagnosis with brain disease [48, 49]. Development of an effective HER2 targeted radiotherapy has the potential to substantially improve therapeutic outcomes for patients with HER2 + metastatic breast cancer. As antibody drug conjugates are

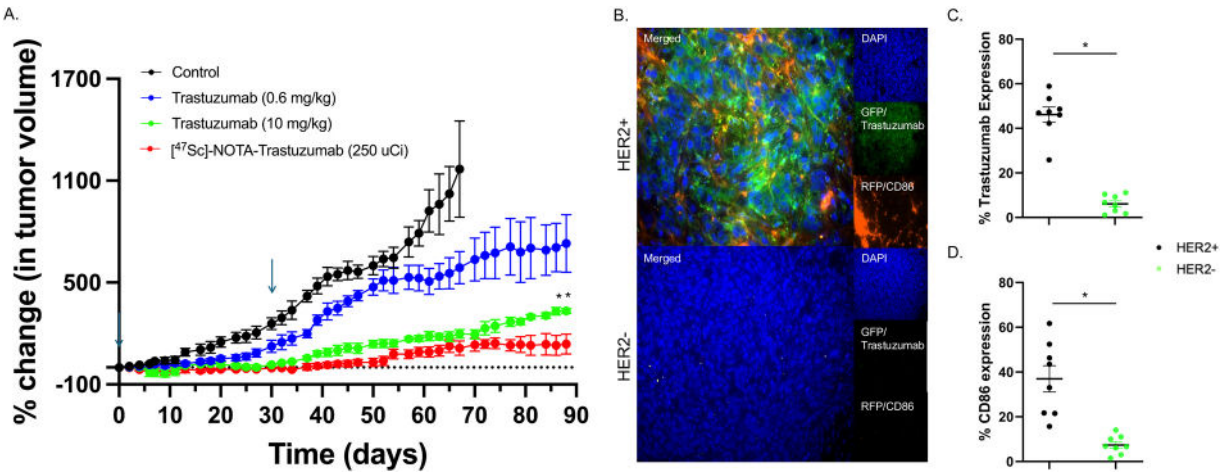

Fig. 5. [^{47}Sc]Sc-NOTA-trastuzumab exhibits greater tumor suppression than 16x cold trastuzumab. Cytotoxicity of [^{47}Sc]Sc-NOTA-trastuzumab was monitored over the course of 60 days and [^{47}Sc]Sc-NOTA-trastuzumab was observed to exhibit a cytostatic effect relative to initial tumor volume (A). Immunofluorescence staining against trastuzumab and CD86 suggest long term tumor suppression from [^{47}Sc]Sc-NOTA-trastuzumab could be the result of increased anti-tumoral activity (B). Quantification of trastuzumab (C) and CD86 expression (D) reveals significant increases in HER2 + cells compared to HER2- cells. Arrows denote the administering of [^{47}Sc]Sc-NOTA-trastuzumab treatment.

well established in the regimens for therapeutic standard of care for HER2 + breast cancer, this study seeks to expand the field by combining antibodies with radionuclide agents, providing treatment synergy and delivery to brain metastases [50,51]. In this study, we developed a targeted radionuclide therapy against HER2 by studying the internalization, localization, and biodistribution of [^{47}Sc]Sc-NOTA--Trastuzumab. This is the first study to develop the radiochemistry and characterize the impact of [^{47}Sc]Sc-NOTA-trastuzumab to treat HER2 + , laying the foundation for clinical application with potential to improve prognosis in late-stage HER2 + disease. Additionally, imaging of the therapy allows characterization of the delivery to treat primary and brain metastatic tumors.

Radionuclide therapy, such as [^{177}Lu]-DOTATATE (Lutathera), has become standard-of-care for treatment in certain solid tumors and has been well tolerated and significantly improves survival in patients [52]. Radionuclide therapy is not currently a part of standard of care in breast cancer [53,54], however [^{177}Lu]Lu-trastuzumab has been investigated for use in patients with HER2 + breast demonstrating high uptake in HER2 + tumors cancer [24]. Still, it was noted that the longitudinal response of HER2 + primary and metastatic breast cancer and the immune response to targeted radionuclide therapy have not been previously observed [24]. In our study, we demonstrate that two doses of [^{47}Sc]Sc-NOTA-trastuzumab (0.6 mg/kg) delivered one month apart have a significant impact on tumor kill and outperform two higher clinical doses of trastuzumab alone. While ^{177}Lu has been used to control tumor growth, ^{47}Sc has potential advantages over currently approved radionuclides [37]. Unlike ^{177}Lu and ^{90}Y, ^{47}Sc has isotopic matching with a positron emitting radionuclide, ^{43}Sc, allowing for matched diagnostic and therapy [55]. Similarly, due to the shorter half-life of ^{47}Sc and low energy beta emission, ^{47}Sc may have a higher therapeutic ratio for small lesions than ^{177}Lu or ^{90}Y, sparing normal tissue and reducing toxicity [56]. Finally, the cyclotron production of ^{47}Sc enables scalable production as an alternative to reactor produced isotopes. Taken together, these advantages highlight the need to evaluate the therapeutic efficacy and biological impact of [47Sc]Sc-based radionuclide therapy in HER2 + breast cancer, particularly given emerging evidence of its effectiveness in other tumor types, including prostate cancer [57].

Metastatic breast cancers are common in patients with advanced late-stage breast cancer, metastasizing to organs like bone, lung, liver and brain [58]. Standard-of-care therapy for unresectable breast-to-brain metastasis consists of whole brain radiotherapy or stereotactic radiation surgery; however, these treatment regimens are limited by off-target effects and size limitations [59]. Trastuzumab has been labeled with chemotherapy to improve delivery and internalization in solid tumors [60,61]. Trastuzumab emtansine (T-DM1) involves linking trastuzumab to the cytotoxic drug, Mertansine, which has been observed to reduce mortality and recurrence by 50%, compared to trastuzumab alone [60]. Similarly, trastuzumab deruxtecan (T-DXD) involves linking trastuzumab to the topoisomerase I inhibitor, deruxtecan, which has be examined in patients with HER2 + metastatic breast cancer and has showed durable antitumoral activity in pretreated patients [62]. It has been preclinically observed that anti-HER2 trastuzumab decreases tumor hypoxia and increases radiosensitization; however, this research is limited to primary, resectable disease [10]. By reducing tumor hypoxia through targeted HER2 antibody trastuzumab, we can sensitize HER2 + lesions to low doses of external beam radiotherapy in HER2 + solid lesions and, by radiolabeling trastuzumab with ^{47}Sc, we increase radionuclide delivery and increase internalization of the ^{47}Sc radionuclide in HER2 + lesions. This is evident in the significant difference in the overall tumor change of the [^{47}Sc]Sc-NOTA--trastuzumab group illustrating enhanced efficacy compared to the trastuzumab treatment groups and the control.

While our study highlights the potential for [^{47}Sc]Sc-NOTA-trastuzumab to be used in patients with HER2 + primary and metastatic disease, our study has limitations. Additionally, there has been significant interest in observing the immunomodulatory effects of radionuclide therapy [63–65]. CD86 staining provides exploratory evidence of increased expression of an M1-associated macrophage marker following [^{47}Sc]Sc-NOTA-trastuzumab therapy; however, CD86 alone does not fully establish macrophage polarization. Future studies incorporating additional markers (such as iNOS, CD80, and MHC-II)will be required to comprehensively define macrophage phenotypes and immune remodeling following targeted radionuclide therapy. Exploring the role of this radiopharmaceutical in a HER2-low model could provide insight into how HER2 expression affects internalization of [^{47}Sc]Sc-NOTA--trastuzumab in the tumor and resulting toxicity [66]. HER2-low (a subset of triple negative) breast cancers encompass approximately 50% of all breast cancer diagnoses and observing how this population of low HER2- expressing cancers responds to [^{47}Sc]-NOTA-trastuzumab could guide clinical decision making [67]. Furthermore, to study the interaction between [^{47}Sc]Sc-NOTA-trastuzumab and adaptive immune cells, an immunocompetent syngeneic model or a humanized model of HER2 + breast cancer could be explored. Yang *et al.* previously observed that [^{177}Lu]-DOTATATE synergizes with CAR T cell therapy to improve

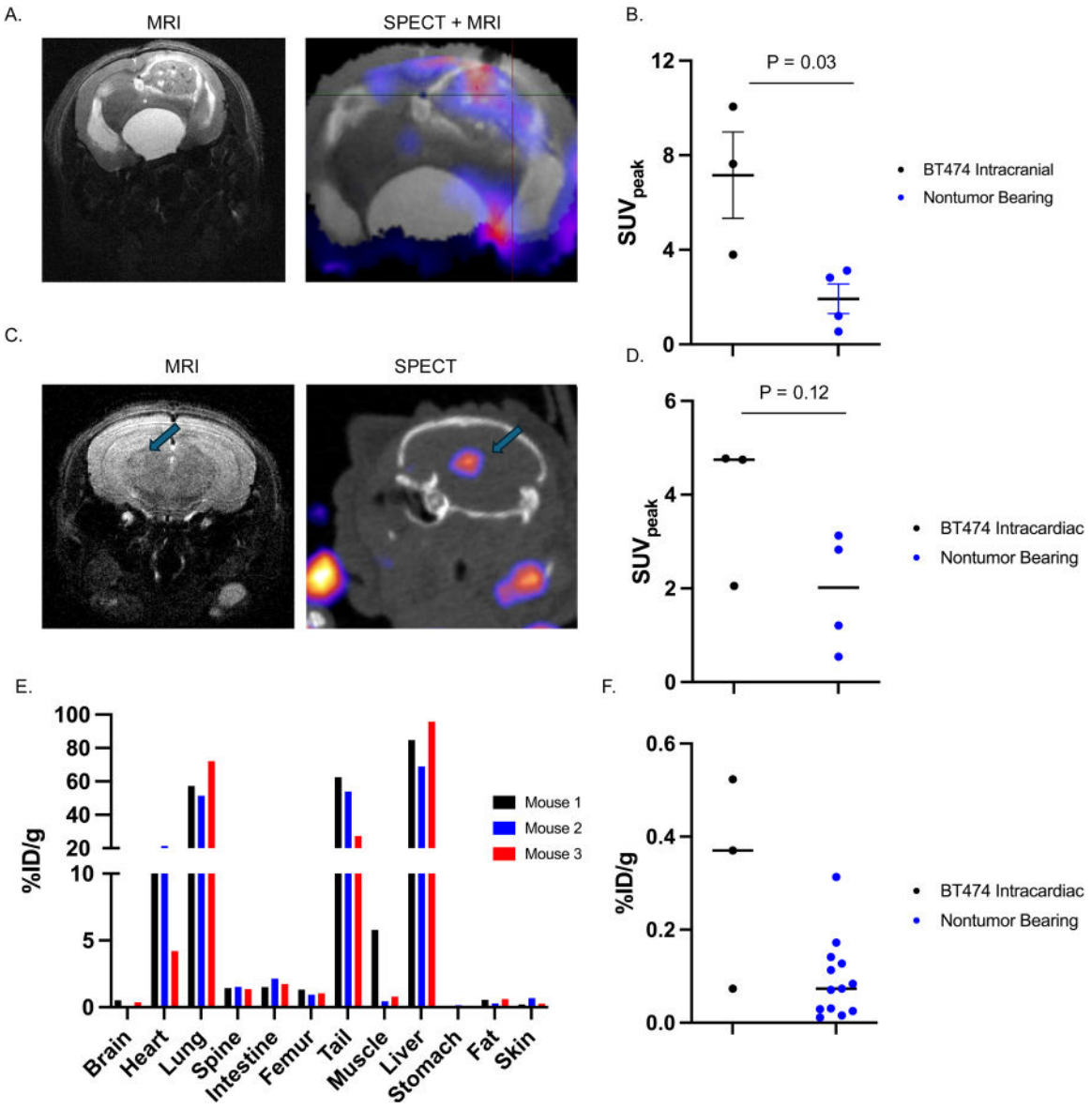

Fig. 6. Exploration of [^{47}Sc]Sc-NOTA-trastuzumab in metastatic models of breast cancer.
To assess the potential for [^{47}Sc]Sc-NOTA-trastuzumab to be utilized in HER2 + brain metastasis, mice with HER2 + intracranial tumors were imaged with [^{47}Sc]Sc-NOTA-trastuzumab and uptake was observed within HER2 + intracranial tumors on day 5 (A, B). Furthermore, SPECT imaging was utilized to image [^{47}Sc]Sc-NOTA-trastuzumab localization in an intracardiac model of HER2 + breast-to-brain disease on day 5 (C, D). Biodistribution analysis suggests increased uptake of [^{47}Sc]Sc-NOTA-trastuzumab was revealed in the lungs and spine (E, F).

tumor control in gastric cancers [68], therefore [^{47}Sc]Sc-NOTA--trastuzumab may have potential to synergize with immunotherapy.

Our study demonstrates that [^{47}Sc]Sc-NOTA-trastuzumab offers high tumor specificity and retention with minimal off-target toxicity. [^{47}Sc]Sc-NOTA-trastuzumab's ability to cross a compromised blood-brain barrier and achieve high tumor uptake with low normal tissue retention suggests a promising metric to target HER2 + brain metastases (in addition to extracranial diseases). By leveraging the synergistic effects of trastuzumab with ^{47}Sc radionuclide therapy, as we are armed with both the therapeutic antibody and the radioisotope, this approach has the potential to enhance the survival for patients with advanced disease. Our findings establish a foundation for future clinical trials and underscore the potential of [^{47}Sc]Sc-NOTA-trastuzumab in advancing targeted radionuclide therapy for HER2-driven cancers.

CRediT authorship contribution statement

Song Patrick: Writing – review & editing, Writing – original draft, Visualization, Methodology, Investigation, Funding acquisition, Formal analysis. **Sharmila Sridhar:** Writing – review & editing, Methodology, Formal analysis. **Cingoranelli Shelbie:** Writing – review & editing, Writing – original draft, Visualization, Methodology, Investigation, Funding acquisition, Formal analysis. **Gallegos Carlos:** Writing – review & editing, Methodology. **Houson Hailey:** Writing – review & editing, Methodology. **Bartels Jennifer:** Writing – review & editing, Methodology. **Watts Lily:** Writing – review & editing, Methodology. **Willey Christopher:** Writing – review & editing, Methodology. **Sorace Anna:** Writing – review & editing, Writing – original draft, Supervision, Project administration, Investigation, Funding acquisition, Formal analysis, Data curation, Conceptualization. **Lapi Suzanne:** Writing – review & editing, Writing – original draft, Supervision, Resources, Project administration, Investigation, Funding acquisition, Formal analysis,

Data curation, Conceptualization.

Declaration of Competing Interest

The authors declare that they have no known competing financial interests or personal relationships that could have appeared to influence the work reported in this paper.

Acknowledgements

This study was supported by DOE Isotope Program (DESC0020197, PI: Lapi) O'Neal Comprehensive Cancer Center, Breast Cancer Research Foundation of Alabama, and National Cancer Institute (R01CA240589, R01CA276540 and R01CA279143, PI: Sorace). The authors would like to thank the UAB Comprehensive Cancer Center's Preclinical Imaging Shared Facility (P30CA013148, S10OD028498-01, and S10OD030465-01). Research reported in this publication was supported by the Alabama Graduate Research Scholars Program (GRSP) funded through the Alabama Commission for Higher Education and administered by the Alabama EPSCoR and National Institute of General Medical Sciences of the National Institutes of Health (Award Number T32GM135028).

Appendix A. Supporting information

Supplementary data associated with this article can be found in the online version at doi:10.1016/j.biopha.2026.119736.

Data Availability

Datasets and materials are available upon reasonable request.

References

[1] C. Liu, et al., Clinical cancer immunotherapy: current progress and prospects, Front. Immunol. 13 (2022) 961805.
[2] A.H. Boekhout, J.H. Beijnen, J.H. Schellens, Trastuzumab, Oncologist 16 (6) (2011) 800–810.
[3] D.L. Costantini, et al., Trastuzumab-resistant breast cancer cells remain sensitive to the auger electron-emitting radiotherapeutic agent 111In-NLS-trastuzumab and are radiosensitized by methotrexate, J. Nucl. Med. 49 (9) (2008) 1498–1505.
[4] J.M. Omweri, et al., Development of (52)Mn labeled trastuzumab for extended time point PET imaging of HER2, Mol. Imaging Biol. 26 (5) (2024) 858–868.
[5] A. Mansur, et al., Quantitative [(89)Zr]Zr-trastuzumab PET and diffusion-weighted MRI for characterization of metastatic HER2-positive breast cancer with PET/MRI, J. Nucl. Med. (2025).
[6] G.A. Ulaner, et al., 89Zr-Trastuzumab PET/CT for detection of human epidermal growth factor receptor 2-positive metastases in patients with human epidermal growth factor receptor 2-negative primary breast cancer, Clin. Nucl. Med. 42 (12) (2017) 912–917.
[7] D.G.J. Linders, et al., 89)Zr-Trastuzumab PET/CT imaging of HER2-positive breast cancer for predicting pathological complete response after neoadjuvant systemic therapy: a feasibility study, Cancers (Basel) 15 (20) (2023).
[8] A. Mansur, et al., Quantitative [(89)Zr]Zr-trastuzumab PET and diffusion-weighted MRI for characterization of metastatic HER2-positive breast cancer with PET/MRI, J. Nucl. Med. 66 (7) (2025) 1018–1026.
[9] L. Guidi, et al., Antibody-drug conjugates in metastatic breast cancer: sequencing, combinations and resistances, Curr. Opin. Oncol. 36 (6) (2024) 487–494.
[10] P.N. Song, et al., Modulation of the tumor microenvironment with trastuzumab enables radiosensitization in HER2+ breast cancer, Cancers (Basel) 14 (4) (2022).
[11] M.Y. Halyard, et al., Radiotherapy and adjuvant trastuzumab in operable breast cancer: tolerability and adverse event data from the NCCTG Phase III Trial N9831, J. Clin. Oncol. 27 (16) (2009) 2638–2644.
[12] M.A. Cobleigh, et al., Comparison of radiation with or without concurrent trastuzumab for HER2-positive ductal carcinoma in situ resected by lumpectomy: a phase III clinical trial, J. Clin. Oncol. 39 (21) (2021) 2367–2374.
[13] K.A. Ahmed, et al., Radiation therapy followed by intrathecal trastuzumab-pertuzumab for ERBB2-positive breast leptomeningeal disease: a phase 1 nonrandomized controlled trial, JAMA Oncol. 10 (7) (2024) 984–986.
[14] E.H. Bent, M.J. Morris, Prostate cancer radioligand therapy: PSMA and beyond, current landscape and future directions, Curr. Oncol. Rep. 27 (10) (2025) 1170–1184.
[15] B. Ahmed, P. Ravi, Current and future perspectives on radioligand therapy in advanced prostate cancer, Ther. Adv. Med. Oncol. 18 (2026) 17588359251409047.
[16] K. Sandhu, et al., PSMA theranostics in prostate cancer and beyond: current and future perspectives, Cancers (Basel) 17 (22) (2025).
[17] H. Dadgar, et al., Targeted radioligand therapy: physics and biology, internal dosimetry and other practical aspects during (177)Lu/(225)Ac treatment in neuroendocrine tumors and metastatic prostate cancer, Theranostics 15 (10) (2025) 4368–4397.
[18] G. Belge Bilgin, et al., Current and future directions in theranostics for neuroendocrine prostate cancer, Cancer Treat. Rev. 136 (2025) 102941.
[19] Y. Liu, et al., Radionuclide therapy of HER2-expressing xenografts using [(177)Lu] Lu-ABY-027 affibody molecule alone and in combination with trastuzumab, Cancers (Basel) 15 (9) (2023).
[20] T.T. Hoang, et al., Delta-like ligand 3-directed (225)Ac radioimmunotherapy in neuroendocrine lung and prostate cancer models, J. Nucl. Med. (2026).
[21] A. Loor, et al., Minimal chemical modification enables alpha/beta radiolabeling of sacituzumab govitecan for targeted therapy in high grade serous ovarian cancer, Eur. J. Nucl. Med. Mol. Imaging (2026).
[22] S.E. Lapi, et al., Recent advances and impending challenges for the radiopharmaceutical sciences in oncology, Lancet Oncol. 25 (6) (2024) e236–e249.
[23] S.M. Larson, et al., Radioimmunotherapy of human tumours, Nat. Rev. Cancer 15 (6) (2015) 347–360.
[24] M. Guleria, et al., Formulation and clinical translation of [(177)Lu]Lu-trastuzumab for radioimmunotheranostics of metastatic breast cancer, RSC Med. Chem. 12 (2) (2021) 263–277.
[25] N. Vinod, et al., Combination of (131)I-trastuzumab and lanatoside C enhanced therapeutic efficacy in HER2 positive tumor model, Sci. Rep. 11 (1) (2021) 12871.
[26] M. Kondo, et al., [(225)Ac]Ac- and [(111)In]In-DOTA-trastuzumab theranostic pair: cellular dosimetry and cytotoxicity in vitro and tumour and normal tissue uptake in vivo in NRG mice with HER2-positive human breast cancer xenografts, EJNMMI Radiopharm. Chem. 8 (1) (2023) 24.
[27] R. Meredith, et al., Dose escalation and dosimetry of first-in-human alpha radioimmunotherapy with 212Pb-TCMC-trastuzumab, J. Nucl. Med. 55 (10) (2014) 1636–1642.
[28] H.A. Houson, et al., PET imaging expedites detection of aberration in the humanization of an annexin A1 targeting antibody, Pharmaceuticals (Basel) 18 (3) (2025).
[29] G.R. Gimblet, et al., PET imaging of differentiated thyroid cancer with thyrotropin-alfa, Sci. Rep. 15 (1) (2025) 11375.
[30] C. Meyer, et al., Tandem isotope therapy with (225)Ac- and (177)Lu-PSMA-617 in a murine model of prostate cancer, J. Nucl. Med. 64 (11) (2023) 1772–1778.
[31] H.A. Houson, et al., PET imaging of the neurotensin targeting peptide NOTA-NT-20.3 using cobalt-55, copper-64 and gallium-68, Pharmaceutics 14 (12) (2022).
[32] S.J. Cingoranelli, et al., Cross section measurements for the production of (49,51) Cr and (47)Sc from proton irradiation of natural vanadium up to 24 MeV, Appl. Radiat. Isot. 212 (2024) 111469.
[33] I. Carbo-Bague, et al., Evaluation of a novel hexadentate 1,2-hydroxypyridinone-based acyclic chelate, HOPO-O(6)-C4, for (43)Sc/(47)Sc, (68)Ga, and (45)Ti radiopharmaceuticals, Nucl. Med. Biol. 128-129 (2024) 108872.
[34] S.J. Cingoranelli, et al., Production and purification of (43)Sc and (47)Sc from enriched [(46)Ti]TiO(2) and [(50)Ti]TiO(2) targets, Sci. Rep. 13 (1) (2023) 22683.
[35] J.A. O'Donoghue, et al., Pharmacokinetics, biodistribution, and radiation dosimetry for (89)Zr-trastuzumab in patients with esophagogastric cancer, J. Nucl. Med. 59 (1) (2018) 161–166.
[36] S.K. Woo, et al., Development of (64)Cu-NOTA-Trastuzumab for HER2 targeting: a radiopharmaceutical with improved pharmacokinetics for human studies, J. Nucl. Med. 60 (1) (2019) 26–33.
[37] S.J. Cingoranelli, et al., Production of high purity (47)Sc from proton irradiation of natural vanadium targets, EJNMMI Radiopharm. Chem. 9 (1) (2024) 89.
[38] S.J. Cingoranelli, et al., Investigating the theranostic potential of elementally matched [(43)Sc]Sc-PSMA-617 and [(47)Sc]Sc-PSMA-617. Mol Pharm, 2026.
[39] T. Lindmo, et al., Determination of the immunoreactive fraction of radiolabeled monoclonal antibodies by linear extrapolation to binding at infinite antigen excess, J. Immunol. Methods 72 (1) (1984) 77–89.
[40] P.N. Song, et al., Dual anti-HER2/EGFR inhibition synergistically increases therapeutic effects and alters tumor oxygenation in HNSCC, Sci. Rep. 14 (1) (2024) 3771.
[41] C.A. Gallegos, et al., Quantitative dynamic granzyme B PET imaging to characterize novel combination immunotherapy response in preclinical glioblastoma models, Theranostics 16 (6) (2026) 2649–2664.
[42] C.A. Gallegos, et al., 89)Zr]-CD8 immunoPET imaging of glioblastoma multiforme response to combination oncolytic viral and checkpoint inhibitor immunotherapy reveals CD8 infiltration differential changes in preclinical models, Theranostics 14 (3) (2024) 911–923.
[43] M.J. Bloom, et al., Quantifying the effects of combination trastuzumab and radiation therapy in human epidermal growth factor receptor 2-positive breast cancer, Cancers (Basel) 14 (17) (2022).
[44] A. Mansur, et al., Combination therapy with trastuzumab and niraparib: quantifying early proliferative alterations in HER2+ breast cancer models, Biomedicines 11 (8) (2023).
[45] A.V.F. Massicano, et al., 89)Zr]-atezolizumab-PET imaging reveals longitudinal alterations in PDL1 during therapy in TNBC preclinical models, Cancers (Basel) 15 (10) (2023).
[46] C.C. Parker, et al., Evaluation of a CD206-targeted peptide for PET imaging of macrophages in syngeneic mouse models of cancer, Mol. Pharm. 20 (5) (2023) 2415–2425.
[47] G. Giordano, et al., Multidisciplinary management of HER2-positive breast cancer with brain metastases: an evidence-based pragmatic approach moving from pathophysiology to clinical data, Crit. Rev. Oncol. Hematol. 192 (2023) 104185.

[48] M. Yakar, D. Etiz, Prognostic factors of breast cancer brain metastasis, World J. Clin. Oncol. 15 (1) (2024) 5–8.
[49] K. Riecke, et al., Long-term survival of breast cancer patients with brain metastases: subanalysis of the BMBC registry, ESMO Open. 8 (3) (2023) 101213.
[50] P. Ma, et al., High risks adverse events associated with trastuzumab emtansine and trastuzumab deruxtecan for the treatment of HER2-positive/mutated malignancies: a pharmacovigilance study based on the FAERS database, Expert. Opin. Drug. Saf. 22 (8) (2023) 685–696.
[51] J. Cortes, et al., Trastuzumab deruxtecan versus trastuzumab emtansine in HER2-positive metastatic breast cancer: long-term survival analysis of the DESTINY-Breast03 trial, Nat. Med. 30 (8) (2024) 2208–2215.
[52] L. Urso, et al., Lutathera((R)) orphans: state of the art and future application of radioligand therapy with (177)Lu-DOTATATE, Pharmaceutics 15 (4) (2023).
[53] O. Sartor, et al., Lutetium-177-PSMA-617 for metastatic castration-resistant prostate cancer, N. Engl. J. Med. 385 (12) (2021) 1091–1103.
[54] R. McBean, et al., Lu177-PSMA therapy for men with advanced prostate cancer: Initial 18 months experience at a single Australian tertiary institution, J. Med. Imaging Radiat. Oncol. 63 (4) (2019) 538–545.
[55] M. Chernysheva, et al., Accelerator production of scandium radioisotopes: Sc-43, Sc-44, and Sc-47, Curr. Radiopharm. 14 (4) (2021) 359–373.
[56] K. Siwowska, et al., Therapeutic potential of (47)Sc in comparison to (177)Lu and (90)Y: preclinical investigations, Pharmaceutics 11 (8) (2019).
[57] S.J. Cingoranelli, et al., Investigating the theranostic potential of elementally matched [(43)Sc]Sc-PSMA-617 and [(47)Sc]Sc-PSMA-617, Mol. Pharm. 23 (3) (2026) 1517–1528.
[58] T.J. Honkanen, et al., Immune cell profiles of metastatic HER2-positive breast cancer patients according to the sites of metastasis, Breast Cancer Res. Treat. 191 (2) (2022) 443–450.
[59] E. Ippolito, et al., Radiotherapy for HER 2 positive brain metastases: urgent need for a paradigm shift, Cancers (Basel) 14 (6) (2022).
[60] E.P. Mamounas, et al., Adjuvant T-DM1 versus trastuzumab in patients with residual invasive disease after neoadjuvant therapy for HER2-positive breast cancer: subgroup analyses from KATHERINE, Ann. Oncol. 32 (8) (2021) 1005–1014.
[61] E. Rassy, L. Rached, B. Pistilli, Antibody drug conjugates targeting HER2: Clinical development in metastatic breast cancer, Breast 66 (2022) 217–226.
[62] S. Modi, et al., Trastuzumab deruxtecan in previously treated HER2-positive breast cancer, N. Engl. J. Med. 382 (7) (2020) 610–621.
[63] R.B. Patel, et al., Low-dose targeted radionuclide therapy renders immunologically cold tumors responsive to immune checkpoint blockade, Sci. Transl. Med. 13 (602) (2021).
[64] H.K. Potluri, et al., Antitumor efficacy of (90)Y-NM600 targeted radionuclide therapy and PD-1 blockade is limited by regulatory T cells in murine prostate tumors, J. Immunother. Cancer 10 (8) (2022).
[65] C.A. Ferreira, et al., Immunomodulatory effects of alpha vs beta radiopharmaceutical therapy in murine prostate cancer, Front. Immunol. 16 (2025) 1563387.
[66] M. Yang, et al., Clinicopathological characteristics of HER2-low breast cancer: a retrospective study, Sci. Rep. 13 (1) (2023) 12382.
[67] Y. Shirman, S. Lubovsky, A. Shai, HER2-low breast cancer: current landscape and future prospects, Breast Cancer (Dove Med Press) 15 (2023) 605–616.
[68] Y. Yang, et al., Low-dose targeted radionuclide therapy synergizes with CAR T cells and enhances tumor response, Front. Immunol. 15 (2024) 1355388.